



Article

# Flavonoids with Glutathione Antioxidant Synergy: Influence of Free Radicals Inflow

Igor Ilyasov <sup>1,\*</sup>, Vladimir Beloborodov <sup>1</sup>, Daniil Antonov <sup>1</sup>, Anna Dubrovskaya <sup>1</sup>, Roman Terekhov <sup>1</sup>, Anastasiya Zhevlakova <sup>1</sup>, Asiya Saydasheva <sup>1</sup>, Vladimir Evteev <sup>2</sup>  and Irina Selivanova <sup>1</sup>

<sup>1</sup> Department of Chemistry, Sechenov First Moscow State Medical University, Trubetskaya Str. 8/2, 119991 Moscow, Russia; Beloborodov\_v\_l@staff.sechenov.ru (V.B.); Antonov\_d\_o@student.sechenov.ru (D.A.); anna.mma@list.ru (A.D.); terekhov\_r\_p@staff.sechenov.ru (R.T.); Zhevlakova\_a\_k@staff.sechenov.ru (A.Z.); Saydasheva\_a\_n@student.sechenov.ru (A.S.); Selivanova\_i\_a@staff.sechenov.ru (I.S.)

<sup>2</sup> Federal State Budgetary Institution “Scientific Centre for Expert Evaluation of Medicinal Products” of the Ministry of Health of the Russian Federation, Petrovsky blvd. 8/2, 127051 Moscow, Russia; Evteev@expmed.ru

\* Correspondence: ilyasov\_i\_r@staff.sechenov.ru; Tel.: +7-985-764-0744

Received: 2 July 2020; Accepted: 28 July 2020; Published: 3 August 2020



**Abstract:** This report explores the antioxidant interaction of combinations of flavonoid–glutathione with different ratios. Two different 2,2′-azino-bis(3-ethylbenzothiazoline-6-sulfonic acid radical (ABTS<sup>•+</sup>)-based approaches were applied for the elucidation of the antioxidant capacity of the combinations. Despite using the same radical, the two approaches employ different free radical inflow systems: An instant, great excess of radicals in the end-point decolorization assay, and a steady inflow of radicals in the lag-time assay. As expected, the flavonoid–glutathione pairs showed contrasting results in these two approaches. All the examined combinations showed additive or light subadditive antioxidant capacity effects in the decolorization assay. This effect showed slight dilution dependence and did not change when the initial ABTS<sup>•+</sup> concentration was two times as high or low. However, in the lag-time assay, different types of interaction were detected, from subadditivity to considerable synergy. Taxifolin–glutathione combinations demonstrated the greatest synergy, at up to 112%; quercetin and rutin, in combination with glutathione, revealed moderate synergy in the 30–70% range; while morin–glutathione appeared to be additive or subadditive. In general, this study demonstrated that, on the one hand, the effect of flavonoid–glutathione combinations depends both on the flavonoid structure and molar ratio; on the other hand, the manifestation of the synergy of the combination strongly depends on the mode of inflow of the free radicals.

**Keywords:** glutathione; taxifolin; quercetin; rutin; morin; ABTS; antioxidant activity; synergistic effect

## 1. Introduction

As a theoretical consideration, a combination of two or more antioxidants might form a “complex network” with cooperative component interactions [1–3]. Thus, deviations of the experimentally derived antioxidant capacities from the theoretically calculated values can be observed, giving rise to the synergistic or subadditive (also known as antagonistic or negative synergistic) effects. Apparently, this phenomenon can substantially influence foods, nutrients, and pharmaceuticals as well as biological systems. Despite the potential sophistication of the antioxidant “complex network” systems, the elementary model of the interaction is a binary combination.

As well as flavonoids, which are common components of fruits, vegetables, tea, herbs, and wine and reveal a wide variety of biological activities [4–7], glutathione can be supplied by foods [8] or

supplements, thus improving glutathione status [9–12]. Glutathione ( $\gamma$ -L-glutamyl-L-cysteinyl-glycine, GSH)—a tripeptide found in most living cells from bacteria to mammals [13]—is the classical scavenging antioxidant which is essential for protecting hepatocytes, erythrocytes, and other cells against toxic injury via enzymatic and nonenzymatic reactions; it acts with electrophilic xenobiotics as a low-molecular-weight detoxifier, transition metals chelator, redox-mediator of proteins' posttranslational modification by glutathionylation, etc. [14–18]. The relatively high glutathione concentration (millimolar range) together with the high ratio of glutathione/glutathione disulfide (GSH/GSSG) in healthy cells (more than 98% of the reduced form) makes the GSSG/GSH redox couple the principal cellular redox buffer and the indicator of the cellular redox state/antioxidant defense against oxidative/nitrosative stress and radiation damage [18–21]. An important factor to consider is the possible flavonoid–glutathione interaction in food/beverages or taken as food supplements and in therapeutic products. However, the effect of their co-presence on each other's biological activity, including antioxidant activity (AOA), is not yet completely understood.

Here, we focused on the elucidation of the antioxidant capacity of flavonoid–glutathione binary combinations. We employed different flavonoid/GSH ratios—from equal to a great excess of GSH. Although the total dietary flavonoid intake can be greater than GSH, the expected concentration of individual flavonoids in an organism is always much less than GSH [8,22–31].

Quercetin, rutin (a glycoside of quercetin), morin (a structural isomer of quercetin), and taxifolin (a reduced form of quercetin) were used as flavonoid components for the combinations (see Figure 1). These flavonoids are well-known natural antioxidants whose potential health benefits have attracted a great deal of interest in their studies as prospective drugs [7,32–39]. Thus, a large and growing body of literature has been devoted to the modification of their biopharmaceutical and physicochemical properties, such as antioxidant activity and bioavailability, by crystal engineering [40–44], obtaining solid dispersions [45–49], and the development of new polymorphic forms [50–54]. This report is in line with the abovementioned works and aims to study the possible alteration of the antioxidant activity of flavonoids by combining them with other natural antioxidants. Instead of applying completely different antioxidant assays, which often result in unrelated and even controversial data that are difficult to interpret, we focused on two different 2,2'-azino-bis[3-ethylbenzothiazoline-6-sulfonic acid radical (ABTS<sup>•+</sup>) radical-cation scavenging approaches based on the decolorization end-point or lag-time experimental strategies [55,56].

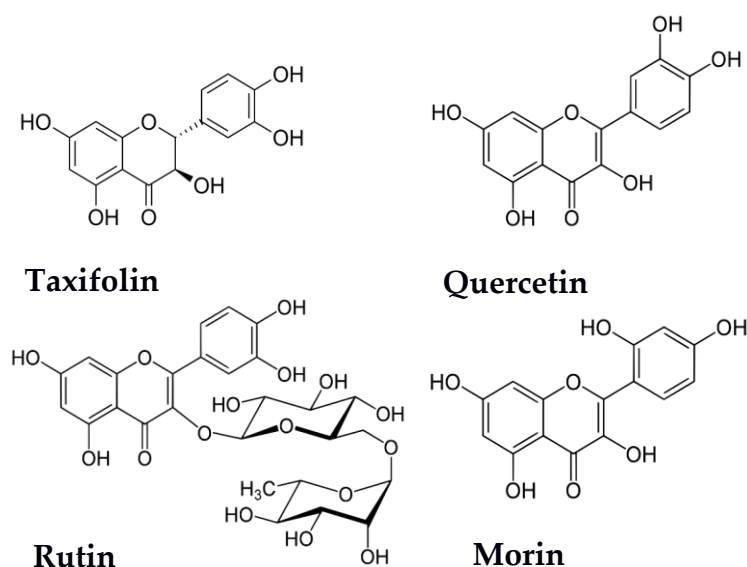


**Figure 1.** Structures of flavonoids; components of the studied combinations.

## 2. Materials and Methods

### 2.1. Materials

#### 2.1.1. Components of Flavonoid–Glutathione Combinations

Taxifolin (LLC “Flavir”, Irkutsk, Russia), reduced glutathione (GSH) and morin were purchased from Sigma-Aldrich Chemie GmbH, Steinheim, Germany. Rutin was purchased from Merck, Darmstadt, Germany; quercetin was purchased from Asha Organics, Geel, Belgium.

#### 2.1.2. Reagents

ABTS, 2,2'-azinobis(3-ethylbenzothiazoline-6-sulfonic acid) diammonium salt, potassium persulfate (di-potassium peroxydisulfate, PP), *N,N*-dimethylformamide and the components of phosphate buffer saline pH 7.0 (PBS)—i.e., dipotassium hydrogen phosphate, potassium dihydrogen phosphate and sodium chloride—were obtained from Sigma-Aldrich. High performance liquid chromatography (HPLC)-grade ethanol and *N,N*-dimethylformamide (puriss.) were obtained from Merck Ltd., Germany and JSC LenReactiv, Russia, respectively.

All reagents were prepared on the day of use. Stock solutions of taxifolin, quercetin, and morin were prepared in ethanol; rutin was initially dissolved in a small amount of *N,N*-dimethylformamide and then ethanol (solvent ratio 1:10) and GSH in deionized water. None of the solvents interfered with the assays.

### 2.2. Methods

Spectrophotometric measurements were performed on a Cary 100 spectrophotometer (Varian, Palo Alto, CA, USA) with a 1 cm Peltier temperature-controlled cuvette.

#### 2.2.1. Decolorization Assay

**General procedure.** The decolorization assay was performed as reported by Re et al. [56] with minor modifications. Briefly, the antioxidant solution was added to the pre-generated ABTS<sup>•+</sup>, shaken intensively for 15 s and placed in a heating chamber at 30 °C for up to 30 min in the dark. The addition of antioxidants led to the characteristic ABTS<sup>•+</sup> maxima of absorption decreasing, which were read at 730 nm at the first, 10th, 15th, 20th, 25th, and 30th minute. The appropriate initial ABTS<sup>•+</sup> absorbance without antioxidants was adjusted to 1.00 ± 0.05 for all measurements and read for each sample just before the addition of antioxidants. The quercetin–glutathione 1:5 combination was additionally tested at 0.05, 0.75, and 2.0 ABTS<sup>•+</sup> initial absorbance to elucidate the influence of ABTS<sup>•+</sup> concentration on the observed antioxidant capacity.

**Generation of ABTS<sup>•+</sup>.** To generate ABTS<sup>•+</sup>, the water stock solutions of ABTS and PP were mixed to final concentrations of 7 mM and 2.5 mM, respectively, and allowed to stand at room temperature overnight. The stock ABTS<sup>•+</sup> was then used for 1–2 days (kept at a storage temperature of 5 °C).

**ABTS<sup>•+</sup> self-bleaching.** We examined the radical–cation self-bleaching of ABTS<sup>•+</sup> at concentrations giving different initial absorbances—from 0.5 to 2.0—at 730 nm. After dilution of a corresponding volume of stock ABTS<sup>•+</sup> in PBS, the initial absorbance and then at 1, 10, 15, 20, 25, and 30 min was measured.

***n*-value and mixture effect calculations.** The decrease in the ABTS<sup>•+</sup> absorbance  $\Delta A$  and the inhibition percentage of ABTS<sup>•+</sup>, Inh%, were calculated applying the following equations:

$$\Delta A = A_0 - A_1 - \Delta A_{\text{self-bleaching}} \quad (1)$$

$$\text{Inh}\% = 100\% \times \Delta A/A_0, \quad (2)$$

where  $A_0$  and  $A_1$  are the  $ABTS^{\bullet+}$  absorbances at 730 nm, a pathlength 1 cm at a zero time-point and after a certain time of incubation with antioxidant (antioxidant mixture), respectively. The self-bleaching of  $ABTS^{\bullet+}$   $\Delta A_{\text{self-bleaching}}$  was calculated as the difference between the  $ABTS^{\bullet+}$  absorbance at a zero time-point and after a certain time of incubation without antioxidant.

The amount of  $ABTS^{\bullet+}$  radicals scavenged by one molecule of antioxidant ( $n$ -value) in the decolorization assay was calculated as follows:

$$n\text{-value} = C_{ABTS^{\bullet+}}/C_{\text{antioxidant}} = \Delta A/\varepsilon \times C_{\text{antioxidant}} \times l, \quad (3)$$

where  $C_{ABTS^{\bullet+}}$  is the concentration of the scavenged  $ABTS^{\bullet+}$ ,  $\varepsilon$  is the extinction coefficient at 15,000 L $\cdot$ mol $^{-1}$  $\cdot$ cm $^{-1}$  (at 730 nm),  $l$  is the optical pathlength of 1 cm and  $C_{\text{antioxidant}}$  is the concentration of antioxidant.

The mixture effect,  $ME$ , was calculated in two ways:

1. The “traditionally calculated mixture effect”:

$$ME_{\text{traditional}} = (\Delta A_{\text{experimental}}^{\text{mix}} - \Delta A_{\text{theoretical}}^{\text{mix}}) \times 100\% / \Delta A_{\text{theoretical}}^{\text{mix}}, \quad (4)$$

where  $\Delta A_{\text{experimental}}^{\text{mix}}$  and  $\Delta A_{\text{theoretical}}^{\text{mix}}$  were calculated as follows:

$$\Delta A_{\text{experimental}}^{\text{mix}} = A_{\text{mix}_0}^{\text{mix}} - A_{30}^{\text{mix}} + \Delta A_{\text{self-bleaching}} \quad (5)$$

$$\Delta A_{\text{theoretical}}^{\text{mix}} = A_{\text{mix}_0}^{\text{mix}} - (A_{30}^1 + A_{30}^2 - A_0) + \Delta A_{\text{self-bleaching}} \quad (6)$$

where  $A_{30}^1$  and  $A_{30}^2$  is the absorbance at the 30th min of component 1 and component 2, respectively, and  $A_{\text{mix}_0}^{\text{mix}}$  is the initial absorbance of the mixture of these components.

2. The “Webb’s simulation mixture effect” [57]:

$$ME_{\text{Webb's simulation}} = (\text{Inh}\%_{\text{experimental}}^{\text{mix}} - \text{Inh}\%_{\text{Webb's simulation}}) \times 100\% / \text{Inh}\%_{\text{Webb's simulation}}, \quad (7)$$

where  $\text{Inh}\%_{\text{experimental}}^{\text{mix}}$  and  $\text{Inh}\%_{\text{Webb's simulation}}$  were calculated as follows:

$$\text{Inh}\%_{\text{experimental}}^{\text{mix}} = 100\% \bullet \Delta A_{\text{experimental}}^{\text{mix}} / A_{\text{mix}_0}^{\text{mix}} \quad (8)$$

$$\text{Inh}\%_{\text{Webb's simulation}} = [1 - (1 - \text{Inh}\%_{\text{flavonoid}}/100) \times (1 - \text{Inh}\%_{\text{glutathione}}/100)] \times 100\%. \quad (9)$$

### 2.2.2. Lag-Time Assay

**General procedure.** The lag-time assay was performed as reported by Ilyasov et al. [55]. Briefly, a solution of PP was added to the antioxidant and ABTS solution in PBS, and then the  $ABTS^{\bullet+}$  absorbance was continuously read until  $ABTS^{\bullet+}$  accumulation recommenced and became steady.

The kinetics of the  $ABTS^{\bullet+}$  accumulation were monitored at maxima of 730 nm with an incubation temperature of  $22 \pm 1$  °C. For each measurement, 4–50  $\mu$ L of antioxidant stock solution was added to 3.3 mL of ABTS dissolved in PBS, and then the reaction was started by the addition of 0.7 mL of PP dissolved in PBS with subsequent intensive shaking for 15 s; final concentrations of ABTS and PP were 1.21 mM and 0.43 mM. In the absence of antioxidants, the accumulation of  $ABTS^{\bullet+}$  began as soon as the PP was added. Normally, absorbance reached  $1.25 \pm 0.05$  by the 15th min of incubation and continually increased for several hours. When an antioxidant was added, the lag-time was usually observed before the  $ABTS^{\bullet+}$  accumulation commenced. The antioxidant concentrations were adjusted to induce a lag-time of not less than 3 min in order to decrease the influence of preparatory time error.

**$n$ -value and mixture effect calculations.** The amount of  $ABTS^{\bullet+}$  radicals scavenged by one molecule of antioxidant ( $n$ -value) for the lag-time assay results was calculated as follows:

$$n\text{-value} = C_{\text{expected } ABTS^{\bullet+}} / C_{\text{antioxidant}}, \quad (10)$$

where  $C_{\text{expected ABTS}^{\bullet+}}$  is the expected accumulated concentration of  $\text{ABTS}^{\bullet+}$ , which corresponds to a certain lag-time, and  $C_{\text{antioxidant}}$  is the concentration of antioxidant.

The expected accumulated  $\text{ABTS}^{\bullet+}$  concentration was calculated from an averaged kinetic curve, which was obtained from seven independent runs (see Figure 2a), considering an  $\text{ABTS}^{\bullet+}$  radical-cation  $\lambda_{\text{max}}$  of 730 nm and  $\epsilon$  at  $15,000 \text{ L}\cdot\text{mol}^{-1}\cdot\text{cm}^{-1}$ .

The mixture effect was calculated in two ways:

- The first one was the traditional method, which took into account the lag-time duration, giving the “lag-time mixture effect”:

$$\text{ME}_{\text{lag-time}} = [(\text{lag-time}_{\text{experimental}} - \text{lag-time}_{\text{theoretical}})/\text{lag-time}_{\text{theoretical}}] \times 100\%, \quad (11)$$

where  $\text{lag-time}_{\text{experimental}}$  is the experimentally derived lag-time duration of the examined combination, in min;  $\text{lag-time}_{\text{theoretical}}$  is the calculated sum of lag-times of individual components of the examined combination, in min.

- The second was calculated through the absolute  $\text{ABTS}^{\bullet+}$  concentration scavenged by antioxidants compared with the expected accumulated  $\text{ABTS}^{\bullet+}$  amount, giving the “scavenged  $\text{ABTS}^{\bullet+}$  mixture effect”.

$$\text{ME}_{\text{scavenged ABTS}^{\bullet+}} = [(C_{\text{expected ABTS}^{\bullet+}}_{\text{experimental}} - C_{\text{expected ABTS}^{\bullet+}}_{\text{theoretical}})/C_{\text{expected ABTS}^{\bullet+}}_{\text{theoretical}}] \times \%, \quad (12)$$

where  $C_{\text{expected ABTS}^{\bullet+}}_{\text{experimental}}$  and  $C_{\text{expected ABTS}^{\bullet+}}_{\text{theoretical}}$  were calculated from the corresponding lag-times applying the averaged kinetic curve (Figure 2a) and taking  $\epsilon$  as  $15,000 \text{ L}\cdot\text{mol}^{-1}\cdot\text{cm}^{-1}$ .

### 2.3. Statistics

The results are shown as the mean ( $\pm$  standard deviation) of at least three determinations. The paired Student's *t*-test was used for the analysis of experimental and simulation results. The R-squared statistics and the F-test of overall significance were used for regression analysis.

## 3. Results

### 3.1. Antioxidant Capacity in the Decolorization Assay

The original protocol of the decolorization assay, which is based on the discoloration of pre-generated  $\text{ABTS}^{\bullet+}$  radical-cations by antioxidants [56], was modified in this work: The initial  $\text{ABTS}^{\bullet+}$  absorbance was increased from 0.7 to 1.0, and the incubation time was extended from 4–6 min to 30 min. Thus, an additional methodology adjustment was performed for clarity regarding the contribution of  $\text{ABTS}^{\bullet+}$  self-bleaching to the measured antioxidant capacity, the influence of different initial  $\text{ABTS}^{\bullet+}$  absorbances on the antioxidant effect of individual compounds and combinations and the susceptibility to different orders of the addition of components of a mixture effect. After that, the individual compounds and flavonoid–glutathione combinations were examined.

#### 3.1.1. Methodology Adjustment

**$\text{ABTS}^{\bullet+}$  self-bleaching.** The  $\text{ABTS}^{\bullet+}$  radical-cation absorbance decrease-time curves demonstrated gradual self-bleaching, which depended very little on the initial concentration of  $\text{ABTS}^{\bullet+}$  and was almost equal by the 15th minute and thereafter in all experiments (see Table S1). The relative rate of self-bleaching decreased to being almost negligible by the 30th minute in all cases, but the absolute cumulative absorbance loss ( $\Delta\text{Abs}$ ) was quite noticeable; i.e., 0.056, 0.061, 0.075, and 0.079 at an initial absorbance of 0.5, 0.75, 1.0 and 2.0 at 730 nm, respectively. This self-bleaching contribution was adjusted to all further antioxidant-mediated absorbance decrease measurement results.

**Antioxidant capacity measurement at different initial ABTS<sup>•+</sup> absorbance.** To compare the relative antioxidant capacity of antioxidants, we calculated the number of ABTS<sup>•+</sup> radicals scavenged by one molecule of antioxidant (*n*-value). At the initial ABTS<sup>•+</sup> absorbance of 1.0 absorbance units, this parameter showed no dependence on the concentration of antioxidants by the 30th minute, except for morin and glutathione, for which the *n*-value dependence on AO concentration was statistically significant, although the absolute *n*-value shift was insufficient.

The *n*-values for quercetin at different initial ABTS<sup>•+</sup> absorbances—i.e., 2.0, 1.0, 0.75, and 0.5—also showed no statistically significant difference.

**Susceptibility to the different ABTS<sup>•+</sup> concentrations of mixture effect.** To evaluate the susceptibility to the different ABTS<sup>•+</sup> concentrations of mixture effect, we tested the same combination (quercetin–glutathione, 1:5) at various absolute and relative concentrations:

- At different reagent concentrations, keeping their ratio the same: quercetin, glutathione and ABTS<sup>•+</sup> at 0.65, 3.26 and 33.3  $\mu$ M, or twice as high—i.e., 1.34, 6.52 and 66.7  $\mu$ M;
- At the same quercetin and glutathione concentrations—i.e., 1.34 and 6.52  $\mu$ M, respectively—but changing ABTS<sup>•+</sup> concentration: 133.2, 66.7, and 50.0  $\mu$ M (with an initial absorbance of 2.0, 1.0, and 0.75, respectively).

All these combinations showed a slight subadditive effect, except for the mixture effect at the initial ABTS<sup>•+</sup> absorbance of 2.0, which appeared to be additive (see Table S2 and Figure S1).

**Susceptibility to the different orders of component addition of the mixture effect.** To elucidate the susceptibility to the sequential addition of components of the mixture effect, we tested the combination of quercetin–glutathione at 1:5. The concentrations of components in the incubation mixture were the same, namely 1.34, 6.52, and 66.7  $\mu$ M for quercetin, glutathione, and ABTS<sup>•+</sup>, respectively. The introduction of components was carried out in two ways:

- Quercetin was mixed with ABTS<sup>•+</sup> and then glutathione was added 1 min later, or vice versa;
- Glutathione was mixed with ABTS<sup>•+</sup> and quercetin was added 1 min later.

In both cases, the mixture effect was subadditive and did not differ from the effect of the combination when both components were added at once (see Table S3 and Figure S2).

### 3.1.2. Individual Compounds

All the tested flavonoids and GSH scavenged ABTS<sup>•+</sup> in a two-phase manner. About 60–70% of the total ABTS<sup>•+</sup> was scavenged during the first-minute fast phase. Then, the inhibition of ABTS<sup>•+</sup> slowed down, leading to the second moderate phase. Nevertheless, on average, 93% and 96% of ABTS<sup>•+</sup> had already been scavenged by the 10th and 15th minute, respectively. By the 30th min, the change in total  $\Delta$ Abs became negligible (see Table 1 and Figure S3). The regression curve slopes rose significantly from 1 to 10 min of incubation; however, they became almost equal by the 20th–30th minute of incubation. The regression curve intercepts were rather low and even insignificant in the case of rutin and taxifolin. The antioxidant capacity of the tested compounds increased in the order glutathione < taxifolin < rutin < morin < quercetin, with *n*-values in the range of 3.5–12.4 (Table 1).

**Table 1.** The *n*-values for flavonoids and glutathione at different incubation times. All *n*-values were statistically different ( $p < 0.05$ ).

Component	<i>n</i> -Value $\pm$ SD (% of the Total <i>n</i> -Value) <sup>1</sup>			
	1 min	10 min	20 min	30 min
Taxifolin	4.0 $\pm$ 0.4 (59.8 $\pm$ 4.3%)	6.1 $\pm$ 0.5 (93.6 $\pm$ 3.1%)	6.5 $\pm$ 0.6 (98.5 $\pm$ 1.9%)	6.8 $\pm$ 0.6
Quercetin	8.9 $\pm$ 1.0 (71.9 $\pm$ 5.5%)	11.1 $\pm$ 0.9 (93.7 $\pm$ 1.4%)	11.9 $\pm$ 1.0 (98.5 $\pm$ 0.7%)	12.4 $\pm$ 1.0
Rutin	5.7 $\pm$ 0.7 (60.9 $\pm$ 5.1%)	8.5 $\pm$ 0.7 (93.9 $\pm$ 1.6%)	9.0 $\pm$ 0.7 (98.8 $\pm$ 1.0%)	9.3 $\pm$ 0.6
Morin	7.9 $\pm$ 1.1 (68.9 $\pm$ 4.8%)	10.1 $\pm$ 1.1 (92.2 $\pm$ 2.1%)	11.0 $\pm$ 1.2 (98 $\pm$ 1.0%)	11.5 $\pm$ 1.3
Glutathione	2.3 $\pm$ 0.2 (65.0 $\pm$ 4.2%)	3.1 $\pm$ 0.3 (92.6 $\pm$ 2.6%)	3.4 $\pm$ 0.3 (98.6 $\pm$ 1.5%)	3.5 $\pm$ 0.3

<sup>1</sup> The *n*-value after 30 min incubation was taken as 100%.

### 3.1.3. Flavonoid–Glutathione Combinations at Different Molar Ratios

As with the previously mentioned quercetin–glutathione 1:5, the assessment of rutin–glutathione, taxifolin–glutathione, morin–glutathione, and quercetin–glutathione combinations at different ratios did not reveal considerable differences in terms of mixture effects, demonstrating subadditive interaction from the statistically insignificant value of  $-3\%$  for quercetin–glutathione 1:1 to the maximal  $-14.5\%$  for morin–glutathione 1:10. Webb’s simulation mixture effects were also calculated for comparison and discussion (Table 2, Figure S4).

**Table 2.** Antioxidant mixture effects of the flavonoid–glutathione combinations in the decolorization assay.

Combination Ratio	Traditionally Calculated Mixture Effect, %				Webb’s Simulation Mixture Effect, %			
Taxifolin–glutathione								
1:1.1 (3.8 $\mu\text{M}$ + 4.2 $\mu\text{M}$ )	-11.15	$\pm$	2.76	b	2.92	$\pm$	5.91	a
1:5.2 (1.8 $\mu\text{M}$ + 9.4 $\mu\text{M}$ )	-9.92	$\pm$	3.88	a	2.90	$\pm$	3.67	a
1:9.9 (1.2 $\mu\text{M}$ + 11.9 $\mu\text{M}$ )	-8.74	$\pm$	1.18	b	1.45	$\pm$	1.60	a
1:15.9 (0.7 $\mu\text{M}$ + 11.1 $\mu\text{M}$ )	-8.45	$\pm$	2.17	b	-2.21	$\pm$	2.41	a
Quercetin–glutathione								
1:1.1 (2.3 $\mu\text{M}$ + 2.6 $\mu\text{M}$ )	-2.90	$\pm$	3.44	a	10.62	$\pm$	5.23	b
1:5.0 (1.3 $\mu\text{M}$ + 6.5 $\mu\text{M}$ )	-7.15	$\pm$	3.20	d	4.81	$\pm$	0.29	a
1:9.6 (0.8 $\mu\text{M}$ + 7.7 $\mu\text{M}$ )	-5.64	$\pm$	4.14	a	3.06	$\pm$	6.06	a
1:14.3 (0.7 $\mu\text{M}$ + 10 $\mu\text{M}$ )	-10.51	$\pm$	1.73	a	-2.28	$\pm$	2.68	a
Rutin–glutathione								
1:1.0 (2.2 $\mu\text{M}$ + 2.3 $\mu\text{M}$ )	-12.92	$\pm$	1.67	d	-3.75	$\pm$	2.74	a
1:5.2 (1.4 $\mu\text{M}$ + 7.3 $\mu\text{M}$ )	-8.36	$\pm$	2.44	a	4.92	$\pm$	1.07	a
1:10.4 (0.9 $\mu\text{M}$ + 9.4 $\mu\text{M}$ )	-9.50	$\pm$	3.84	b	0.65	$\pm$	4.59	a
1:15.9 (0.7 $\mu\text{M}$ + 11.1 $\mu\text{M}$ )	-7.98	$\pm$	1.17	b	0.77	$\pm$	1.05	a
Morin–glutathione								
1:1.0 (3.4 $\mu\text{M}$ + 3.4 $\mu\text{M}$ )	-10.13	$\pm$	1.03	a	3.89	$\pm$	1.70	a
1:5.1 (1.5 $\mu\text{M}$ + 7.7 $\mu\text{M}$ )	-12.90	$\pm$	2.94	a	2.37	$\pm$	1.51	a
1:9.6 (1.1 $\mu\text{M}$ + 10.6 $\mu\text{M}$ )	-14.49	$\pm$	1.60	a	-0.61	$\pm$	3.29	a
1:16.1 (0.7 $\mu\text{M}$ + 11.3 $\mu\text{M}$ )	-10.87	$\pm$	3.54	a	0.32	$\pm$	2.54	a

a—statistically insignificant,  $p > 0.05$ ; b, d—statistically significant with  $p$ -values less than 0.05 and 0.001, respectively.

### 3.2. Antioxidant Capacity in the Lag-Time Assay

In contrast to the decolorization assay, this approach is based on the gradual inflow and accumulation of  $\text{ABTS}^{\bullet+}$  radical-cations as a result of the In Situ reaction of ABTS with potassium persulfate. Typically, the introduction of an antioxidant leads to the delay of  $\text{ABTS}^{\bullet+}$  accumulation, resulting in a lag-time whose duration depends on the antioxidant concentration [55].

#### 3.2.1. Individual Compounds

The kinetic curve shapes for all the examined individual compounds were in line with those previously reported for this experimental design [55]. The lag-time durations for individual compounds and combinations were obtained from kinetic curves to calculate  $n$ -values and mixture effects, respectively (Figure 2). The calculated  $n$ -values were as follows: 4.7, 3.3, 2.8, 2.7, and 0.8 for quercetin, morin, rutin, taxifolin, and glutathione, respectively [58]. Combinations of the tested flavonoids with glutathione were shown to have different mixture effects, from subadditive to a considerable synergy, which depended on both the flavonoid component structure and the ratio of components.

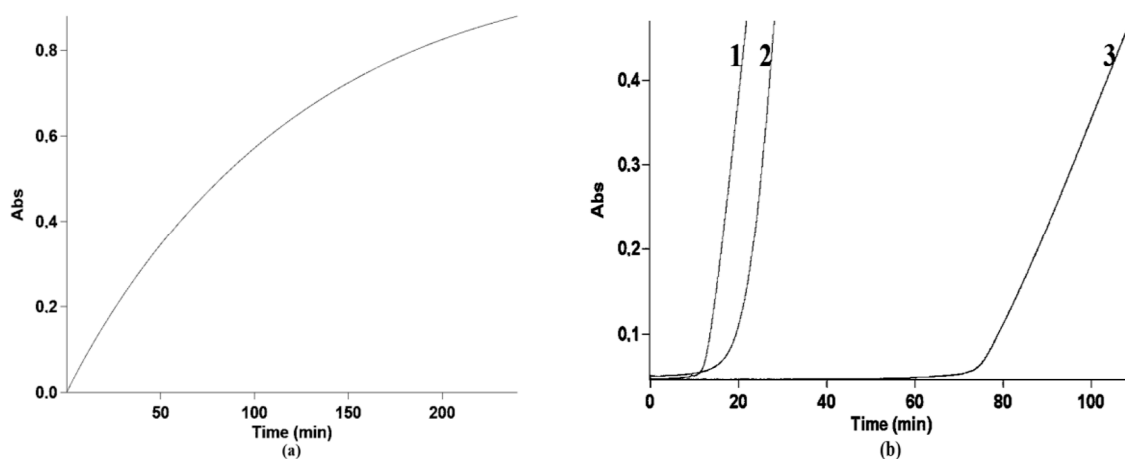


**Figure 2.** The averaged kinetic curves of the 2,2'-azino-bis(3-ethylbenzothiazoline-6-sulfonic acid radical (ABTS•+) accumulation: (a) Without antioxidants or (b) in the presence of taxifolin (1) and glutathione (2), and their combination at a ratio of 1:8 (3). (a) Averaged from seven runs at the initial concentrations of ABTS and PP of 1.21 mM and 0.43 mM, respectively;  $\lambda$  730 nm, pathlength 0.1 cm. (b) Taxifolin 20  $\mu$ M (1), glutathione 160  $\mu$ M (2), and their mixture at 20 + 160  $\mu$ M (3), respectively.  $\lambda$  730 nm, pathlength 1 cm.

### 3.2.2. Flavonoid–Glutathione Combinations at Different Molar Ratios

**Taxifolin–glutathione.** All the tested taxifolin and glutathione combinations, except for the 1:1 ratio, demonstrated significant synergy. The most considerable effect was observed at ratios from 1:8 to 1:16, with a maximum of 112% at 1:16. This synergy then gradually reduced when the glutathione content was increased but still remained significant at 1:50, amounting to about 70% (see Table 3, Figure S5a).

**Table 3.** Mixture effects of flavonoid–glutathione combinations in the lag-time assay.

Ratio	Lag-Time Mixture Effect, %				Scavenged ABTS•+ Mixture Effect, %			
Taxifolin–glutathione								
1:1 (40 $\mu$ M + 40 $\mu$ M)	21.47	±	7.05	b	12.85	±	5.3	a
1:4 (10 $\mu$ M + 40 $\mu$ M)	52.35	±	6.19	c	43.61	±	5.41	c
1:8 (10 $\mu$ M + 80 $\mu$ M)	101.67	±	4.47	d	81.89	±	3.39	d
1:12 (10 $\mu$ M + 120 $\mu$ M)	108.19	±	6.46	c	83.23	±	5.63	c
1:16 (10 $\mu$ M + 160 $\mu$ M)	111.57	±	10.24	c	81.96	±	7.52	c
1:20 (10 $\mu$ M + 200 $\mu$ M)	94.49	±	3.1	d	66.86	±	2.14	d
1:30 (10 $\mu$ M + 300 $\mu$ M)	84.93	±	9.21	c	52.48	±	5.81	c
1:50 (10 $\mu$ M + 500 $\mu$ M)	69.55	±	5.84	c	34.49	±	2.37	c
Quercetin–glutathione								
1:4 (10 $\mu$ M + 40 $\mu$ M)	30.72	±	14.44	a	21.94	±	12.08	a
1:8 (5 $\mu$ M + 40 $\mu$ M)	34.71	±	10.97	b	26.62	±	9.92	b
1:12 (5 $\mu$ M + 60 $\mu$ M)	44.01	±	8.56	b	32.99	±	7.14	b
1:16 (5 $\mu$ M + 80 $\mu$ M)	51.28	±	9.21	b	38.38	±	8.55	b
1:20 (5 $\mu$ M + 100 $\mu$ M)	40.40	±	7.92	b	28.22	±	5.58	b
Rutin–glutathione								
1:2.5 (16 $\mu$ M + 40 $\mu$ M)	62.55	±	16.04	b	48.45	±	13.51	b
1:5 (8 $\mu$ M + 40 $\mu$ M)	70.84	±	17.57	b	58.11	±	14.94	b
1:7.5 (8 $\mu$ M + 60 $\mu$ M)	65.80	±	3.23	d	52.17	±	2.33	d
1:10 (8 $\mu$ M + 80 $\mu$ M)	70.36	±	8.39	c	54.48	±	6.83	c
1:12.5 (8 $\mu$ M + 100 $\mu$ M)	67.76	±	8.46	c	51.26	±	6.83	c
Morin–glutathione								
1:4 (10 $\mu$ M + 40 $\mu$ M)	−3.30	±	1.13	b	−6.84	±	0.98	c
1:8 (5 $\mu$ M + 40 $\mu$ M)	−4.51	±	8.25	a	−7.34	±	7.7	a
1:12 (5 $\mu$ M + 60 $\mu$ M)	−3.50	±	1.73	a	−6.46	±	1.77	b
1:16 (5 $\mu$ M + 80 $\mu$ M)	−3.60	±	2.24	a	−6.56	±	2.19	b
1:20 (5 $\mu$ M + 100 $\mu$ M)	−6.52	±	3.04	a	−7.32	±	3.78	a

a—statistically insignificant,  $p > 0.05$ ; b, c, d—statistically significant with  $p$ -values less than 0.05, 0.01 and 0.001, respectively.

**Quercetin–glutathione.** Quercetin with glutathione also demonstrated synergy. Again, the observed synergy rose with the glutathione content, increasing up to the 1:16 ratio and then declining. The general magnitude of synergy was less considerable than in the case of taxifolin–glutathione combinations with a maximum value which was around half the size, at 51% (see Table 3, Figure S5b).

**Rutin–glutathione.** The combinations of rutin with glutathione revealed a significant synergy which generally did not depend on the component ratio. The magnitude of the mixture effect at all the examined ratios was almost the same and averaged  $68 \pm 11\%$  (see Table 3, Figure S5c).

**Morin–glutathione.** The only combination which showed no synergy was morin–glutathione. As in the case of the rutin–glutathione combinations, no dependence of the mixture effect on the component ratio was revealed. Additive and slight subadditive mixture effects were observed at different component ratios (see Table 3, Figure S5d).

## 4. Discussion

Despite the tendency in recent years to assess the antioxidant capacity utilizing completely different methods in parallel, there are certain problems in interpreting the obtained results. In this work, we tried to apply different approaches while utilizing the same antioxidants and—more importantly—the same model radicals. There are numerous methods to measure antioxidant activity/antioxidant capacity (AOA/AOC) [3,59–67]; of those, the ABTS-based methods are among the most widely used [58]. We applied two approaches based on the scavenging of  $\text{ABTS}^{\bullet+}$  radical-cations to evaluate the antioxidant interaction of flavonoid–glutathione combinations. However, several methodological considerations needed to be taken into account.

### 4.1. Methodological Considerations

#### 4.1.1. Decolorization Assay

Approaches based on the  $\text{ABTS}^{\bullet+}$  discoloration have certain shortcomings which have been discussed multiple times to date [68–70]. One of them is ascribed to the different interlaboratory values of antioxidant capacities obtained for the same antioxidants. This can be related to complicated kinetic patterns, elevated stoichiometries and the dependence of the relative antioxidant capacity (e.g., the Trolox equivalent antioxidant capacity (TEAC) index) on antioxidant concentration [55,71–73]. As a result of unfinished  $\text{ABTS}^{\bullet+}$  inhibition in the presence of antioxidants by the 4th, 6th, or even 30th minute [74–80], the ambiguity of the obtained data complicates their interpretation.

This impelled us to explore the optimal end-point—i.e., the incubation time when the radical inhibition has almost completed—before we proceeded to the elucidation of mixture effects. Our experiments showed that a 15–20 min incubation time turned out to be sufficient for all the tested AOs; by this time, all of them showed 96–99% of the total antioxidant capacity, even though the decrease in  $\text{ABTS}^{\bullet+}$  still continued after 30 min of incubation at rates which were negligibly higher than self-bleaching. Since we focused on the elucidation of antioxidant capacity, we decided to adjust the starting  $\text{ABTS}^{\bullet+}$  absorbance to  $1.0 \pm 0.5$  instead of  $0.7 \pm 0.5$  as used the original procedure [56]. Thus, we could use a wider range of antioxidant concentrations, as recommended by Tian and Schaich [72]. This was important for the combinations and allowed us to avoid making the lowest component concentration too low—i.e., difficult to measure in terms of the decrease of  $\text{ABTS}^{\bullet+}$ —and at the same time allowed us to work in the optimal spectrophotometer absorbance range.

Additionally, we determined  $\text{ABTS}^{\bullet+}$  self-bleaching parameters to account for their contribution to all measured antioxidant capacity results. In contrast to our expectations, they turned out to be slightly different at various initial  $\text{ABTS}^{\bullet+}$  absorbances, resulting in  $\text{ABTS}^{\bullet+}$  absorbance loss due to self-bleaching in the range from  $0.056 \pm 0.0014$  to  $0.079 \pm 0.0025$  by the 30th minute. However, the  $\text{ABTS}^{\bullet+}$  absorbance decrease rates were very close at different initial  $\text{ABTS}^{\bullet+}$  concentrations—and by the 15th minute became indistinguishable—which shows that the initial difference could be

due to dissolved oxygen or traces of metals which after reacting with  $\text{ABTS}^{\bullet+}$  ceased to influence its self-bleaching.

The number of  $\text{ABTS}^{\bullet+}$  radicals scavenged by one molecule of antioxidant, the  $n$ -value, turned out to be an extremely useful parameter to estimate the relative antioxidant capacity as it showed the stoichiometry result of the interaction of  $\text{ABTS}^{\bullet+}$  with antioxidants. In our opinion, the lack of dependence—or slight dependence—of the same antioxidant  $n$ -values on concentrations in most of our experiments might be attributed not to the specific nature of the AOs but to the narrow  $\text{ABTS}^{\bullet+}$  inhibition concentration ranges tested (10–40 inh%). In contrast, morin and glutathione were both tested in a wider range (10–60 inh%) and as a result showed a statistically significant inversely proportional decrease in  $n$ -value. Apparently, the higher the  $\text{ABTS}^{\bullet+}$ :antioxidant ratio, the deeper the interaction; previously, it has been shown that the reaction of antioxidants with  $\text{ABTS}^{\bullet+}$  can be deeper when the latter is in excess [58]. However, this effect was mostly negligible. The intercepts of regression curves were small and mostly did not differ significantly from zero, which means that we reached the completion of the reaction at all the tested concentrations and therefore avoided the concentration-dependence of relative antioxidant capacity (Figure S3).

The parameter conventionally used for ABTS-based assays, the  $\text{ABTS}^{\bullet+}$  inhibition percentage (%inh), was shown to be less reliable than the absolute absorbance loss ( $\Delta\text{Abs}$ ) or the  $n$ -value. For instance, the  $\Delta\text{Abs}$  did not differ at various initial  $\text{ABTS}^{\bullet+}$  absorbances (in the range of 0.5–2.0 absorbance units) for the same quercetin concentration, which was quite logical: A certain amount of quercetin can scavenge up to a certain amount of  $\text{ABTS}^{\bullet+}$ , independent of the total  $\text{ABTS}^{\bullet+}$  concentration. Indeed, when the  $\text{ABTS}^{\bullet+}$  solutions with absorbances of 1.0 or 2.0 were treated with the same amount of quercetin (with a final concentration of 1.34  $\mu\text{M}$ ), the absolute absorbance loss did not differ, at  $0.25 \pm 0.02$  and  $0.27 \pm 0.02$  absorbance units, respectively, but the calculated inhibition percentages appeared to be  $24.6 \pm 1.35\%$  and  $13.2 \pm 0.63\%$ , respectively. The latter result can be confusing and even misleading, meaning that the %inh parameter only works correctly if one keeps the initial absorbance at one point, allowing only minimum deviations. Thus, we based our calculations on the  $\Delta\text{Abs}$  values and calculated  $n$ -values.

#### 4.1.2. Lag-Time Assay

The time interval between the start of incubation and the accumulation of  $\text{ABTS}^{\bullet+}$ —the lag-time parameter—which is usually used in this type of assays was shown to be contradictory in terms of reliability. The reason for this was that the lags in our experiments appeared to be rather long and the rate of  $\text{ABTS}^{\bullet+}$  accumulation and its change therefore began to matter. Normally, the lag time for different experiment durations can be comparable if the same events happen at the same periods during the whole period of lag. In our case, this could be only possible if the rate of radical generation changed insufficiently. For example, 5 min of lag-time from the second to seventh minute in comparison to the period from the 52nd to 57th minute is supposed to imply the scavenging of the same number of free radicals; in this case, lag-time duration is a reliable parameter. Of course, that was not the case in our assay, as the  $\text{ABTS}^{\bullet+}$  accumulation rate changed to an extent which cannot be ignored (Figure 2a); thus, we decided to modify this parameter.

We therefore transformed the lag-time duration into the  $\text{ABTS}^{\bullet+}$  concentration, which was expected to accumulate by the end of every certain lag-time, giving the “Scavenged  $\text{ABTS}^{\bullet+}$  mixture effect”. Undoubtedly, this method has shortcomings; most importantly, the rate of  $\text{ABTS}^{\bullet+}$  generation can technically speaking be influenced by antioxidants, and we assumed that this influence was absent or negligible. Despite this, this approach is much more reliable, although it considerably decreased the calculated synergy for combinations (Table 3). On the other hand, this allowed us to avoid the overestimation of mixture effects; thus, we can state with certainty that combinations for which we observed considerable synergy are synergistic, irrespective of the calculation or simulation approaches.

#### 4.2. Evaluation of the Antioxidant Capacity of Individual Compounds

Both in the decolorization assay and lag-time assay, the antioxidant capacity of individual compounds demonstrated the expected general tendency, with glutathione and quercetin revealing the lowest and the highest scavenging activity, respectively. However, the absolute amount of ABTS<sup>•+</sup> molecules captured by one molecule of antioxidant was different. In the decolorization assay, this was excessive both in the case of flavonoids or glutathione and could be ascribed to the occurrence of various sideline reactions. Flavonoids demonstrated high *n*-values even after 1 min of incubation (for example, almost nine molecules of ABTS<sup>•+</sup> per molecule of quercetin). The glutathione *n*-value after 1 min incubation—2.3 ABTS<sup>•+</sup> molecules—was also far from the physiologically plausible stoichiometric factor 1 and reached 3.5 ABTS<sup>•+</sup> molecules by the 30th min. The latter might be explained by the oxidation of glutathione not only to glutathione disulfide but further to sulfinic/sulfenic/sulfonic acids or to the formation of adducts with ABTS<sup>•+</sup> and was previously observed by several authors [55,80–84]. Moreover, it was recently demonstrated that ABTS<sup>•+</sup> bleaching by glutathione disulfide substantially evolves at the elevated temperatures [84].

For the lag-time assay, the *n*-values appeared to be much more adequate. Presumably, the antioxidant/ABTS<sup>•+</sup> ratio plays a critical role here. In the decolorization assay, the ABTS<sup>•+</sup> is in great excess, leading to high stoichiometries and stimulating all the possible reactions with ABTS<sup>•+</sup>. In the lag-time assay, the opposite situation—i.e., an excess of antioxidant during lag-time and gradual inflow of ABTS<sup>•+</sup>—results in more plausible stoichiometries for most of the examined antioxidants. The recently published review on the reaction pathways involved in the ABTS/PP assay has shed some light on the possible reasons for the high stoichiometries [58]. Apparently, phenolics are not only oxidized when treated by ABTS<sup>•+</sup> but also form coupling adducts, which can undergo further oxidative degradation, with the formation of hydrazinediylidene-like and imine-like adducts [85–94]. The complex biphasic pattern reported previously [72,80,95–97] suggests the fact that oxidation intermediates of antioxidants subsequently capture ABTS<sup>•+</sup> radical-cations, thus elevating the total antioxidant capacity; moreover, their contribution can be rather substantial [78].

#### 4.3. Evaluation of the Antioxidant Capacity of Flavonoid–Glutathione Combinations

The chemistry of antioxidant effect of a certain antioxidant is presumably obvious: An antioxidant reacts with a free radical thus reducing it, and in its turn is supposed to get converted into a low-reactive oxidized form (neutral or radical). Radical scavenging is a high rate process; regarding, the absolute amounts of reacting species, this process could be observed to be similar to, for example, an acid-base interaction. Obviously, no matter whether sodium hydroxide alone reacts with hydrochloric acid or in a mixture with another alkali, if the acid is in excess, sodium hydroxide neutralizes the same amount of acid, and the stoichiometry does not change. This situation is generally reproduced by various total antioxidant capacity assays, where the total effect of a mixture can be predicted by summing effects of individual compounds in it. The total stoichiometry of a reaction for an antioxidant might not be influenced by a second antioxidant apart from the case when the antioxidants or their oxidized forms interact between themselves. This might lead to different transformations: If the low-reacting sites are converted to high-reacting ones, or a stronger antioxidant is regenerated by the so-called “sacrificial” antioxidant, the synergistic action is observed, and vice versa for subadditivity.

We calculated synergistic or subadditive effects for combinations by simply comparing their effects with the sum of the antioxidant capacities of their components, as previously done using different antioxidant capacity assays [98–106]. In the decolorization assay, the antioxidant capacity of individual compounds generally demonstrated a linear dependence on concentration. The interaction stoichiometry varied insufficiently at different concentrations of both radical or antioxidant: This was demonstrated on the example of quercetin at different concentrations, or the same quercetin concentration with different initial ABTS<sup>•+</sup> radical-cations concentrations. Furthermore, in the lag-time assay, there are no sensible limits for lag-time duration; thus, we avoided using the sophisticated

calculations sometimes applied for mixture effect estimations, which have been mostly focused on drugs or enzyme-related compounds, such as Webb's method or similar [57,100,107–110].

Actually, the results for all the tested combinations in the decolorization assay were discouraging. Of course, we could speculate about the tendencies and subtle differences between flavonoid combinations and the various ratios of combinations observed (Table 2), but they all were in such a narrow range that the mean value for all the tested combinations' subadditive effect, at  $-9\%$ , had a standard deviation of only  $\pm 3\%$ . Similar to our results, additive or usually light subadditive antioxidant effects were observed when applying end-point ABTS<sup>•+</sup>-based decolorization assays; e.g., for different combinations of various phenolics [102]; a wide set of different antioxidants, such as ascorbic acid, glutathione, quercetin, and uric acid [81]; human blood plasma combined with flavonoids, incl. quercetin and rutin [111]; binary and ternary mixtures of gallic, ferulic and caffeic acids [112]; and flavonoids and ascorbic acid [113]. Two possible reasons for this subadditivity manifestation were proposed: The formation of non-reactive adducts and regeneration of less active antioxidants by more active antioxidants [81]. In addition, we hypothesized that a sufficient excess of ABTS<sup>•+</sup> in the decolorization assay incubation medium could prevent most of the possible interactions between components, as the short-living flavoxyl or glutathionyl radicals were much more likely to meet ABTS<sup>•+</sup> radicals than each other.

This prompted us to examine the cause of the inconsiderable subadditivity, and we suggest that the cause was the methodology design. To check this hypothesis, the lag-time assay was applied for the same combinations at different ratios.

In contrast to the decolorization assay, in which we failed to reveal sufficient mixture effects, here we could observe considerable synergy and different tendencies of dependence of the mixture effect on the component ratios (Table 3).

As long as the structurally related flavonoids were considered, namely two flavonols quercetin and morin with different types of hydroxylation of the B ring (catechol-like and resorcinol-like, respectively)—quercetin glycoside rutin, and flavanonol taxifolin—we performed their comparative analysis.

Several tendencies can be regarded as they have different structural fragments in the B and C-rings (Figure 1). The catechol-like hydroxylation of the B-ring is possibly important for the manifestation of synergy in combinations with glutathione. Only in the case of morin, which has a resorcinol-like hydroxylation of the B-ring, was no synergy observed. Taxifolin, whose specific structural feature is the saturated character of the C2–C3 bond and alcohol-like hydroxyl at C3 in the C-ring, demonstrated the most considerable synergy. A little less synergy was found for rutin–glutathione and quercetin–glutathione combinations, at up to 71% and 51%, respectively. Both have a C2–C3 double bond and phenol-like hydroxyl at C3, although this is glycosylated in the case of rutin. The ratio-dependence of the mixture effect was shown for combinations of taxifolin or quercetin with glutathione: The combinations with a moderate prevalence of glutathione content, from 1:8 to 1:16, appeared to be more synergistic (up to 112%). The most pronounced synergy effect in taxifolin–glutathione may be a consequence of the fact that taxifolin has the lowest redox potential and is closest to that of the reversible redox system GSH–GSSG [19,114,115].

#### 4.4. Mixture Effect Manifestation and Calculation Approaches

This is not the first work on the assessment of the antioxidant activity of binary flavonoid–glutathione. Pereira et al. [108] studied mixture effects of various flavonoids with glutathione in another discoloration assay, based on the 2,2-diphenyl-1-picrylhydrazyl radical (DPPH<sup>•</sup>). A possible chemical basis of the subadditive, additive and synergistic effects was suggested and comprehensively discussed as well as probable products of flavonoid–glutathione interaction, which were mainly ascribed to the formation of glutathione adducts with flavonoid quinones, which was discovered previously [116–126]. The authors deduced that the presence of a catechol group in the B ring is essential for synergisms with GSH; this conclusion was partly confirmed in our study as well. However,

there were certain methodological issues; the most important was the sufficient non-linearity of the DPPH• scavenging capacity from antioxidant concentrations observed for both the flavonoids and GSH. This phenomenon was then demonstrated to be common for various other antioxidants in DPPH• assays [127,128]. To overcome its impact on the mixture effect, Webb's simulation was carefully adjusted for all the results: effects from subadditive to synergistic (up to 34%) were calculated. Nonetheless, some uncertainty still persists, as any simulation of this kind might lead to overestimation. The lack of unity in the mixture effect calculation approach is confirmed by the fact that several other researchers who have applied the DPPH• assay to elucidate the effect of combination directly compared the antioxidant capacity of a combination with the theoretical sum of the contribution of its antioxidants, which in turn could lead to its underestimation [129–131]. Here, we tried to avoid the hyperbolic character of our dose–response curves for flavonoids and glutathione by extending the incubation time (up to 30 min) as we were aware of the recently reported possible dependence of antioxidant quenching stoichiometry on its concentration [69,72]. Although we can claim that we succeeded, almost all of our curves might be described by both linear or power functions with very close correlation coefficients (Figure S3). Possibly, we could therefore also apply Webb's simulation for our decolorization assay results, thereafter shifting them towards synergistic effects. Such calculation-dependent alterations of combination effects mean that any statements about synergy or subadditivity need to be confirmed by applying different methods and be widely discussed. That is why as to our opinion, the introduction of any additional complexities such as simulations and the like is better avoided. Likewise, we tended to base all our conclusions regarding the decolorization assay results on traditional calculation approaches. In our case, the lag-time approach was adjusted for combinations as alternative and much more explicit effects (up to 83% or 111% synergy, if different calculation strategies were used) were demonstrated, even though a very rigorous mixture effect calculation approach was applied.

## 5. Conclusions

Here, the influence of the modeled system and apparently favorable conditions for the unhindered manifestation of combination effects were carefully demonstrated. Based on the example of ABTS-based assays, we showed that not only the model radical but also calculation strategies and—most of all—the circumstances under which the radical comes into the incubation medium influence the mixture effect. Namely, the same system consisting of an ABTS•<sup>+</sup> radical–cation and antioxidant combinations was applied in two different ways, each giving totally different results: a great excess of ABTS•<sup>+</sup> from the very beginning of incubation in the end-point decolorization assay, and the steady-inflow of ABTS•<sup>+</sup> to the mixture of antioxidants in the lag-time assay. A considerable ratio-dependent synergistic effect was demonstrated for flavonoids with glutathione, which was up to 112% for taxifolin–glutathione combinations. In summary, the gradual ABTS•<sup>+</sup> inflow allowed the components to interact, thus resulting in high synergies, instead of each component experiencing deeper oxidation separately from each other. It seems that the lag-time strategy can be much more promising in combination effects studies. In contrast, the end-point decolorization assay appeared to be less sensitive to manifestations of mixture effects, therefore suiting the estimation of the total antioxidant capacity of complex combinations.

**Supplementary Materials:** The following are available online at <http://www.mdpi.com/2076-3921/9/8/695/s1>. Figure S1. Susceptibility to different initial ABTS•<sup>+</sup> concentrations of the antioxidant mixture effect in the decolorization assay: 133.3, 66.7 and 50 μM, respectively. Figure S2. Susceptibility to different component addition orders of the antioxidant mixture effect in the decolorization assay. Figure S3. The inhibition of ABTS•<sup>+</sup> by flavonoids and glutathione. Figure S4. Antioxidant mixture effect of flavonoid–glutathione combinations at different ratios in the decolorization assay: taxifolin–glutathione (a,b), quercetin–glutathione (c,d), rutin–glutathione (e,f) and morin–glutathione (g,h). Figure S5. Antioxidant mixture effect of flavonoid–glutathione combinations at different ratios in the lag-time assay: taxifolin–glutathione (a), quercetin–glutathione (b), rutin–glutathione (c) and morin–glutathione (d). Table S1. ABTS•<sup>+</sup> self-bleaching at different initial absorbances. Table S2. Influence of different initial ABTS•<sup>+</sup> concentrations on the antioxidant mixture effect of quercetin–glutathione 1:5 in the decolorization assay. Table S3. Influence of different component addition orders on the antioxidant mixture effect of the quercetin–glutathione 1:5 combination in the decolorization assay

**Author Contributions:** Conceptualization, I.I. and V.B.; methodology, I.I. and V.B.; data curation, D.A., A.D., R.T., A.Z. and A.S.; investigation, I.I., D.A., A.D., R.T., A.Z., A.S. and V.E.; formal analysis, I.I., D.A., R.T., A.Z., A.S. and V.E.; resources, V.B. and I.S.; writing—original draft preparation, I.I., D.A.; writing—review and editing, I.I., V.B., D.A., R.T., V.E. and I.S.; visualization, D.A., R.T., A.Z., A.S. and V.E.; supervision, I.I.; project administration, V.B. and I.S. All authors have read and agreed to the published version of the manuscript.

**Funding:** This research was funded by the Russian Academic Excellence Project 5-100.

**Conflicts of Interest:** The authors declare no conflict of interest.

## References

1. Wang, S.; Zhu, F. Dietary antioxidant synergy in chemical and biological systems. *Crit. Rev. Food Sci. Nutr.* **2017**, *57*, 2343–2357. [[CrossRef](#)] [[PubMed](#)]
2. Ingold, K.U. Inhibition of the Autoxidation of Organic Substances in the Liquid Phase. *Chem. Rev.* **1961**, *61*, 563–589. [[CrossRef](#)]
3. Ingold, K.U.; Pratt, D.A. Advances in Radical-Trapping Antioxidant Chemistry in the 21st Century: A Kinetics and Mechanisms Perspective. *Chem. Rev.* **2014**, *114*, 9022–9046. [[CrossRef](#)] [[PubMed](#)]
4. Valavanidis, A.; Vlachogianni, T. Plant polyphenols: Recent advances in epidemiological research and other studies on cancer prevention. In *Studies in Natural Products Chemistry*; Elsevier: Amsterdam, The Netherlands, 2013; pp. 269–295.
5. Spencer, J.P.E.; Crozier, A. (Eds.) *Flavonoids and Related Compounds*; CRC Press: Boca Raton, FL, USA, 2012.
6. Fernandes, I.; Pérez-Gregorio, R.; Soares, S.; Mateus, N.; de Freitas, V. Wine Flavonoids in Health and Disease Prevention. *Molecules* **2017**, *22*, 292. [[CrossRef](#)] [[PubMed](#)]
7. Panche, A.N.; Diwan, A.D.; Chandra, S.R. Flavonoids: An overview. *J. Nutr. Sci.* **2016**, *5*, e47. [[CrossRef](#)]
8. Flagg, E.W.; Coates, R.J.; Eley, J.W.; Jones, D.P.; Gunter, E.W.; Byers, T.E.; Block, G.S.; Greenberg, R.S. Dietary glutathione intake in humans and the relationship between intake and plasma total glutathione level. *Nutr. Cancer* **1994**, *21*, 33–46. [[CrossRef](#)]
9. Richie, J.P.; Nichenametla, S.; Neidig, W.; Calcagnotto, A.; Haley, J.S.; Schell, T.D.; Muscat, J.E. Randomized controlled trial of oral glutathione supplementation on body stores of glutathione. *Eur. J. Nutr.* **2015**, *54*, 251–263. [[CrossRef](#)]
10. Minich, D.M.; Brown, B.I. A Review of Dietary (Phyto)Nutrients for Glutathione Support. *Nutrients* **2019**, *11*, 2073. [[CrossRef](#)]
11. Sinha, R.; Sinha, I.; Calcagnotto, A.; Trushin, N.; Haley, J.S.; Schell, T.D.; Richie, J.P., Jr. Oral supplementation with liposomal glutathione elevates body stores of glutathione and markers of immune function. *Eur. J. Clin. Nutr.* **2018**, *72*, 105–111. [[CrossRef](#)]
12. Park, E.Y.; Shimura, N.; Konishi, T.; Sauchi, Y.; Wada, S.; Aoi, W.; Nakamura, Y.; Sato, K. Increase in the Protein-Bound Form of Glutathione in Human Blood after the Oral Administration of Glutathione. *J. Agric. Food Chem.* **2014**, *62*, 6183–6189. [[CrossRef](#)]
13. Hamilton, C.J.; Arbach, M.; Groom, M. Beyond Glutathione: Different Low Molecular Weight Thiols as Mediators of Redox Regulation and Other Metabolic Functions in Lower Organisms. In *Recent Advances in Redox Active Plant and Microbial Products*; Springer: Dordrecht, The Netherlands, 2014; pp. 291–320.
14. Haenen, G.R.M.M.; Bast, A. Glutathione revisited: A better scavenger than previously thought. *Front. Pharmacol.* **2014**, *5*, 260. [[CrossRef](#)]
15. Gupta, P.K. Biotransformation. In *Fundamentals of Toxicology*; Elsevier: Amsterdam, The Netherlands, 2016; pp. 73–85.
16. Drisko, J.A. Chelation Therapy. In *Integrative Medicine*; Elsevier: Amsterdam, The Netherlands, 2018; pp. 1004–1015.
17. Cha, S.J.; Kim, H.; Choi, H.J.; Lee, S.; Kim, K. Protein Glutathionylation in the Pathogenesis of Neurodegenerative Diseases. *Oxidative Med. Cell. Longev.* **2017**, *2017*, 2818565. [[CrossRef](#)]
18. Cooper, A.J.; Pinto, J.T.; Callery, P.S. Reversible and irreversible protein glutathionylation: Biological and clinical aspects. *Expert Opin. Drug Metab. Toxicol.* **2011**, *7*, 891–910. [[CrossRef](#)]
19. Gaucher, C.; Boudier, A.; Bonetti, J.; Clarot, I.; Leroy, P.; Parent, M. Glutathione: Antioxidant Properties Dedicated to Nanotechnologies. *Antioxidants* **2018**, *7*, 62. [[CrossRef](#)]

20. Deponte, M. The Incomplete Glutathione Puzzle: Just Guessing at Numbers and Figures? *Antioxid Redox Signal.* **2017**, *27*, 1130–1161. [[CrossRef](#)]
21. Forman, H.J.; Zhang, H.; Rinna, A. Glutathione: Overview of its protective roles, measurement, and biosynthesis. *Mol. Asp. Med.* **2009**, *30*, 1–12. [[CrossRef](#)]
22. Turck, D.; Bresson, J.; Burlingame, B.; Dean, T.; Fairweather-Tait, S.; Heinonen, M.; Hirsch-Ernst, K.I.; Mangelsdorf, I.; McArdle, H.J.; Naska, A.; et al. Scientific Opinion on taxifolin-rich extract from Dahurian Larch (*Larix gmelinii*). *EFSA J.* **2017**, *15*, e04682.
23. Zherdev, V.; Kolyvanov, G.; Litvin, A.; Sariiev, A.; Kolesnik, Y.; Titova, E.; Tikhonov, V.P.; Shmatkov, D.; Appolonova, S.; Baranov, P. Pharmacokinetics and metabolism of Dihydroquercetin isolated from *Larix sibirica* Ledeb. *Planta Med.* **2008**, *74*, PA331. [[CrossRef](#)]
24. Yang, P.; Xu, F.; Li, H.-F.; Wang, Y.; Li, F.-C.; Shang, M.-Y.; Liu, G.-X.; Wang, X.; Cai, S.-Q. Detection of 191 Taxifolin Metabolites and Their Distribution in Rats Using HPLC-ESI-IT-TOF-MSn. *Molecules* **2016**, *21*, 1209. [[CrossRef](#)]
25. Yang, C.-J.; Wang, Z.-B.; Mi, Y.-Y.; Gao, M.-J.; Lv, J.-N.; Meng, Y.-H.; Yang, B.Y.; Kuang, H.-X. UHPLC-MS/MS Determination, Pharmacokinetic, and Bioavailability Study of Taxifolin in Rat Plasma after Oral Administration of its Nanodispersion. *Molecules* **2016**, *21*, 494. [[CrossRef](#)]
26. Sayre, C.L.; Gerde, K.D.; Yáñez, J.A.; Davies, N.M. Clinical Pharmacokinetics of Flavonoids. In *Flavonoid Pharmacokinetics*; John Wiley & Sons, Inc.: Hoboken, NJ, USA, 2012; pp. 195–247.
27. Kaushik, D.; O'Fallon, K.; Clarkson, P.M.; Patrick Dunne, C.; Conca, K.R.; Michniak-Kohn, B. Comparison of Quercetin Pharmacokinetics Following Oral Supplementation in Humans. *J. Food Sci.* **2012**, *77*, H231–H238. [[CrossRef](#)]
28. Abdelkawy, K.S.; Balyshv, M.E.; Elbarbry, F. A new validated HPLC method for the determination of quercetin: Application to study pharmacokinetics in rats. *Biomed. Chromatogr.* **2017**, *31*, e3819. [[CrossRef](#)] [[PubMed](#)]
29. Vogiatzoglou, A.; Mulligan, A.A.; Lentjes, M.A.H.; Luben, R.N.; Spencer, J.P.E.; Schroeter, H.; Khaw, K.-T.; Kuhnle, G.G.C. Flavonoid Intake in European Adults (18 to 64 Years). *PLoS ONE* **2015**, *10*, e0128132. [[CrossRef](#)] [[PubMed](#)]
30. Cassidy, A.; O'Reilly, É.J.; Kay, C.; Sampson, L.; Franz, M.; Forman, J.P.; Curhan, G.; Rimm, E.B. Habitual intake of flavonoid subclasses and incident hypertension in adults. *Am. J. Clin. Nutr.* **2011**, *93*, 338–347. [[CrossRef](#)]
31. Peterson, J.J.; Dwyer, J.T.; Jacques, P.F.; McCullough, M.L. Improving the estimation of flavonoid intake for study of health outcomes. *Nutr. Rev.* **2015**, *73*, 553–576. [[CrossRef](#)]
32. Shebeko, S.K.; Zupanets, I.A.; Popov, O.S.; Tarasenko, O.O.; Shalamay, A.S. Effects of Quercetin and Its Combinations on Health. In *Polyphenols: Mechanisms of Action in Human Health and Disease*; Elsevier: Amsterdam, The Netherlands, 2018; pp. 373–394.
33. Sunil, C.; Xu, B. An insight into the health-promoting effects of taxifolin (dihydroquercetin). *Phytochemistry* **2019**, *166*, 112066. [[CrossRef](#)]
34. Sharma, S.; Ali, A.; Ali, J.; Sahni, J.K.; Baboota, S. Rutin: Therapeutic potential and recent advances in drug delivery. *Expert Opin. Investig. Drugs* **2013**, *22*, 1063–1079. [[CrossRef](#)]
35. Caselli, A.; Cirri, P.; Santi, A.; Paoli, P. Morin: A Promising Natural Drug. *Curr. Med. Chem.* **2016**, *23*, 774–791. [[CrossRef](#)]
36. Khan, H.; Jawad, M.; Kamal, M.A.; Baldi, A.; Xiao, J.; Nabavi, S.M.; Daglia, M. Evidence and prospective of plant derived flavonoids as antiplatelet agents: Strong candidates to be drugs of future. *Food Chem. Toxicol.* **2018**, *119*, 355–367. [[CrossRef](#)]
37. Shevelev, A.B.; La Porta, N.; Isakova, E.P.; Martens, S.; Biryukova, Y.K.; Belous, A.S.; Sivokhin, D.A.; Trubnikova, E.V.; Zylkova, M.V.; Belyakova, A.V.; et al. In Vivo Antimicrobial and Wound-Healing Activity of Resveratrol, Dihydroquercetin, and Dihydromyricetin against *Staphylococcus aureus*, *Pseudomonas aeruginosa*, and *Candida albicans*. *Pathogens* **2020**, *9*, 296. [[CrossRef](#)]
38. Sthijns, M.M.J.P.E.; Schiffers, P.M.; Janssen, G.M.; Lemmens, K.J.A.; Ides, B.; Vangrieken, P.; Bouwman, F.G.; Mariman, E.C.; Pader, I.; Arnér, E.S.J.; et al. Rutin protects against H<sub>2</sub>O<sub>2</sub>-triggered impaired relaxation of placental arterioles and induces Nrf2-mediated adaptation in Human Umbilical Vein Endothelial Cells exposed to oxidative stress. *Biochim. Biophys. Acta Gen. Subj.* **2017**, *1861*, 1177–1189. [[CrossRef](#)] [[PubMed](#)]

39. Boots, A.W.; Haenen, G.R.M.M.; Bast, A. Health effects of quercetin: From antioxidant to nutraceutical. *Eur. J. Pharmacol.* **2008**, *585*, 325–337. [[CrossRef](#)] [[PubMed](#)]
40. Setyawan, D.; Permata, S.A.; Zainul, A.; Lestari, M.L.A.D. Improvement in vitro Dissolution Rate of Quercetin Using Cocrystallization of Quercetin-Malonic Acid. *Indones. J. Chem.* **2018**, *18*, 531. [[CrossRef](#)]
41. Selivanova, I.A.; Terekhov, R.P. Engineering of Dihydroquercetin Crystals. *Pharm. Chem. J.* **2020**, *53*, 1081–1085. [[CrossRef](#)]
42. Liu, F.; Wang, L.-Y.; Li, Y.-T.; Wu, Z.-Y.; Yan, C.-W. Protective Effects of Quercetin against Pyrazinamide Induced Hepatotoxicity via a Cocrystallization Strategy of Complementary Advantages. *Cryst. Growth Des.* **2018**, *18*, 3729–3733. [[CrossRef](#)]
43. Selivanova, I.A.; Terekhov, R.P. Crystal engineering as a scientific basis for modification of physicochemical properties of bioflavonoids. *Russ. Chem. Bull.* **2019**, *68*, 2155–2162. [[CrossRef](#)]
44. He, H.; Huang, Y.; Zhang, Q.; Wang, J.-R.; Mei, X. Zwitterionic Cocrystals of Flavonoids and Proline: Solid-State Characterization, Pharmaceutical Properties, and Pharmacokinetic Performance. *Cryst. Growth Des.* **2016**, *16*, 2348–2356. [[CrossRef](#)]
45. Kulkarni, A.D.; Belgamwar, V.S. Influence of novel carrier Soluplus® on aqueous stability, oral bioavailability, and anticancer activity of Morin hydrate. *Dry. Technol.* **2019**, *37*, 1143–1161. [[CrossRef](#)]
46. Surampalli, G.; Satla, M.; Nanjwade, B.K.; Patil, P.A. In vitro and in vivo effects of morin on the intestinal absorption and pharmacokinetics of olmesartan medoxomil solid dispersions. *Drug Dev. Ind. Pharm.* **2017**, *43*, 812–829. [[CrossRef](#)]
47. Gilley, A.D.; Arca, H.C.; Nichols, B.L.B.; Mosquera-Giraldo, L.I.; Taylor, L.S.; Edgar, K.J.; Neilson, A.P. Novel cellulose-based amorphous solid dispersions enhance quercetin solution concentrations in vitro. *Carbohydr. Polym.* **2017**, *157*, 86–93. [[CrossRef](#)]
48. Wei, Q.; Keck, C.M.; Müller, R.H. Preparation and tableting of long-term stable amorphous rutin using porous silica. *Eur. J. Pharm. Biopharm.* **2017**, *113*, 97–107. [[CrossRef](#)] [[PubMed](#)]
49. Baranov, I.A.; Dzhons, D.Y.; Budruev, A.V.; Mochalova, A.E.; Smirnova, L.A.; Koryagin, A.S. Long-acting bioactive composition based on chitosan and taxifolin. *Inorg. Mater. Appl. Res.* **2015**, *6*, 479–484. [[CrossRef](#)]
50. Borghetti, G.S.; Carini, J.P.; Honorato, S.B.; Ayala, A.P.; Moreira, J.C.F.; Bassani, V.L. Physicochemical properties and thermal stability of quercetin hydrates in the solid state. *Thermochim. Acta* **2012**, *539*, 109–114. [[CrossRef](#)]
51. Terekhov, R.P.; Selivanova, I.A.; Zhevlakova, A.K.; Porozov, Y.B.; Dzuban, A.V. Analysis of dihydroquercetin physical modification via in vitro and in silico methods. *Biomeditsinskaya Khimiya* **2019**, *65*, 152–158. [[CrossRef](#)] [[PubMed](#)]
52. Yan, T.; Ji, M.; Sun, Y.; Yan, T.; Zhao, J.; Zhang, H.; Wang, Z. Preparation and characterization of baicalein/hydroxypropyl- $\beta$ -cyclodextrin inclusion complex for enhancement of solubility, antioxidant activity and antibacterial activity using supercritical antisolvent technology. *J. Incl. Phenom. Macrocycl. Chem.* **2020**, *96*, 285–295. [[CrossRef](#)]
53. Terekhov, R.P.; Selivanova, I.A.; Tyukavkina, N.A.; Shylov, G.V.; Utenishev, A.N.; Porozov, Y.B. Taxifolin tubes: Crystal engineering and characteristics. *Acta Crystallogr. Sect. B Struct. Sci. Cryst. Eng. Mater.* **2019**, *75*, 175–182. [[CrossRef](#)]
54. Franklin, S.J.; Myrdal, P.B. Solid-State and Solution Characterization of Myricetin. *AAPS PharmSciTech* **2015**, *16*, 1400–1408. [[CrossRef](#)]
55. Ilyasov, I.R.; Beloborodov, V.L.; Selivanova, I.A. Three ABTS•+ radical cation-based approaches for the evaluation of antioxidant activity: Fast- and slow-reacting antioxidant behavior. *Chem. Pap.* **2018**, *72*, 1917–1925. [[CrossRef](#)]
56. Re, R.; Pellegrini, N.; Proteggente, A.; Pannala, A.; Yang, M.; Rice-Evans, C. Antioxidant activity applying an improved ABTS radical cation decolorization assay. *Free Radic. Biol. Med.* **1999**, *26*, 1231–1237. [[CrossRef](#)]
57. Webb, J.L. *Enzyme and Metabolic Inhibitors. Vol.1. General Principles of Inhibition*; Academic Press: New York, NY, USA, 1963; pp. 55–79.
58. Ilyasov, I.R.; Beloborodov, V.L.; Selivanova, I.A.; Terekhov, R.P. ABTS/PP Decolorization Assay of Antioxidant Capacity Reaction Pathways. *Int. J. Mol. Sci.* **2020**, *21*, 1131. [[CrossRef](#)]
59. Gülçin, I. Antioxidant activity of food constituents: An overview. *Arch. Toxicol.* **2012**, *86*, 345–391. [[CrossRef](#)] [[PubMed](#)]
60. Shahidi, F.; Zhong, Y. Measurement of antioxidant activity. *J. Funct. Foods* **2015**, *18*, 757. [[CrossRef](#)]

61. López-Alarcón, C.; Denicola, A. Evaluating the antioxidant capacity of natural products: A review on chemical and cellular-based assays. *Anal. Chim. Acta* **2013**, *763*, 1–10. [[CrossRef](#)] [[PubMed](#)]
62. Apak, R.; Özyürek, M.; Güçlü, K.; Çapanoğlu, E. Antioxidant Activity/Capacity Measurement. 2. Hydrogen Atom Transfer (HAT)-Based, Mixed-Mode (Electron Transfer (ET)/HAT), and Lipid Peroxidation Assays. *J. Agric. Food Chem.* **2016**, *64*, 1028–1045. [[CrossRef](#)]
63. Apak, R.; Özyürek, M.; Güçlü, K.; Çapanoğlu, E. Antioxidant Activity/Capacity Measurement. 1. Classification, Physicochemical Principles, Mechanisms, and Electron Transfer (ET)-Based Assays. *J. Agric. Food Chem.* **2016**, *64*, 997–1027. [[CrossRef](#)]
64. Niki, E. Assessment of antioxidant capacity in vitro and in vivo. *Free Radic. Biol. Med.* **2010**, *49*, 503–515. [[CrossRef](#)]
65. Pellegrini, N.; Vitaglione, P.; Granato, D.; Fogliano, V. Twenty-five years of total antioxidant capacity measurement of foods and biological fluids: Merits and limitations. *J. Sci. Food Agric.* **2019**. [[CrossRef](#)]
66. Li, B.; Pratt, D.A. Methods for determining the efficacy of radical-trapping antioxidants. *Free Radic. Biol. Med.* **2015**. [[CrossRef](#)]
67. Apak, R.; Capanoglu, E.; Shahidi, F. (Eds.) *Measurement of Antioxidant Activity & Capacity. Recent Trends and Applications*; John Wiley & Sons, Ltd.: Chichester, UK, 2018.
68. Cano, A.; Arnao, M.B. ABTS/TEAC (2,2'-azino-bis(3-ethylbenzothiazoline-6-sulfonic acid)/Trolox<sup>®</sup>-Equivalent Antioxidant Capacity) radical scavenging mixed-mode assay. In *Measurement of Antioxidant Activity & Capacity*; John Wiley & Sons, Ltd.: Chichester, UK, 2017; pp. 117–139.
69. Schaich, K.M.; Tian, X.; Xie, J. Hurdles and pitfalls in measuring antioxidant efficacy: A critical evaluation of ABTS, DPPH, and ORAC assays. *J. Funct. Foods* **2015**, *14*, 111–125. [[CrossRef](#)]
70. Apak, R. Current Issues in Antioxidant Measurement. *J. Agric. Food Chem.* **2019**, *67*, 9187–9202. [[CrossRef](#)]
71. van den Berg, R.; Haenen, G.R.M.M.; van den Berg, H.; Bast, A. Applicability of an improved Trolox equivalent antioxidant capacity (TEAC) assay for evaluation of antioxidant capacity measurements of mixtures. *Food Chem.* **1999**, *66*, 511–517. [[CrossRef](#)]
72. Tian, X.; Schaich, K.M. Effects of molecular structure on kinetics and dynamics of Trolox Equivalent Antioxidant Capacity (TEAC) Assay with ABTS +•. *J. Agric. Food Chem.* **2013**, *61*, 5511–5519. [[CrossRef](#)] [[PubMed](#)]
73. Rosen, J.; Than, N.N.; Koch, D.; Poeggeler, B.; Laatsch, H.; Hardeland, R. Interactions of melatonin and its metabolites with the ABTS cation radical: Extension of the radical scavenger cascade and formation of a novel class of oxidation products, C2-substituted 3-indolinones. *J. Pineal. Res.* **2006**, *41*, 374–381. [[CrossRef](#)]
74. Magalhães, L.M.; Segundo, M.A.; Reis, S.; Lima, J.L.F.C. Methodological aspects about in vitro evaluation of antioxidant properties. *Anal. Chim. Acta* **2008**, *613*, 1–19. [[CrossRef](#)] [[PubMed](#)]
75. Klein, O.I.; Kulikova, N.A.; Filimonov, I.S.; Koroleva, O.V.; Konstantinov, A.I. Long-term kinetics study and quantitative characterization of the antioxidant capacities of humic and humic-like substances. *J. Soils Sediments* **2018**, *18*, 1355–1364. [[CrossRef](#)]
76. Zheng, L.; Zhao, M.; Xiao, C.; Zhao, Q.; Su, G. Practical problems when using ABTS assay to assess the radical-scavenging activity of peptides: Importance of controlling reaction pH and time. *Food Chem.* **2016**, *192*, 288–294. [[CrossRef](#)]
77. Takebayashi, J.; Tai, A.; Yamamoto, I. pH-dependent long-term radical scavenging activity of AA-2G and 6-octa-AA-2G against 2,2'-azinobis(3-ethylbenzothiazoline-6-sulfonic acid) radical cation. *Biol. Pharm. Bull.* **2003**, *26*, 1368–1370. [[CrossRef](#)]
78. Arts, M.J.T.J.; Haenen, G.R.M.M.; Voss, H.P.; Bast, A. Antioxidant capacity of reaction products limits the applicability of the Trolox Equivalent Antioxidant Capacity (TEAC) assay. *Food Chem. Toxicol.* **2004**, *42*, 45–49. [[CrossRef](#)]
79. Arts, M.J.T.J.; Sebastiaan Dallinga, J.; Voss, H.P.; Haenen, G.R.M.M.; Bast, A. A new approach to assess the total antioxidant capacity using the TEAC assay. *Food Chem.* **2004**, *88*, 567–570. [[CrossRef](#)]
80. Walker, R.B.; Everette, J.D. Comparative reaction rates of various antioxidants with ABTS radical cation. *J. Agric. Food Chem.* **2009**, *57*, 1156–1161. [[CrossRef](#)]
81. Błaż, A.; Pilaszek, T.; Grzelak, A.; Dragan, A.; Bartosz, G. Interaction between antioxidants in assays of total antioxidant capacity. *Food Chem. Toxicol.* **2008**, *46*, 2365–2368. [[CrossRef](#)] [[PubMed](#)]
82. Giles, G.I.; Jacob, C. Reactive sulfur species: An emerging concept in oxidative stress. *Biol. Chem.* **2002**, *383*, 375–388. [[CrossRef](#)] [[PubMed](#)]

83. Çelik, S.E.; Özyürek, M.; Güçlü, K.; Apak, R. Solvent effects on the antioxidant capacity of lipophilic and hydrophilic antioxidants measured by CUPRAC, ABTS/persulphate and FRAP methods. *Talanta* **2010**, *81*, 1300–1309. [[CrossRef](#)] [[PubMed](#)]
84. Görüşük, E.M.; Bekdeşer, B.; Bener, M.; Apak, R. ABTS radical-based single reagent assay for simultaneous determination of biologically important thiols and disulfides. *Talanta* **2020**, *218*, 121212. [[CrossRef](#)]
85. Osman, A.M.; Wong, K.K.Y.; Hill, S.J.; Fernyhough, A. Isolation and the characterization of the degradation products of the mediator ABTS-derived radicals formed upon reaction with polyphenols. *Biochem. Biophys. Res. Commun.* **2006**, *340*, 597–603. [[CrossRef](#)]
86. Osman, A.M.; Wong, K.K.Y.; Fernyhough, A. ABTS radical-driven oxidation of polyphenols: Isolation and structural elucidation of covalent adducts. *Biochem. Biophys. Res. Commun.* **2006**, *346*, 321–329. [[CrossRef](#)]
87. Matsumura, E.; Yamamoto, E.; Numata, A.; Kawano, T.; Shin, T.; Murao, S. Structures of the Laccase-catalyzed Oxidation Products of Hydroxy-benzoic Acids in the Presence of ABTS [2,2'-Azino-di-(3-ethylbenzothiazoline-6-sulfonic Acid)]. *Agric. Biol. Chem.* **1986**, *50*, 1355–1357. [[CrossRef](#)]
88. Shin, T.; Murao, S.; Matsumura, E. A chromogenic oxidative coupling reaction of laccase: Applications for laccase and angiotensin I converting enzyme assay. *Anal Biochem.* **1987**, *166*, 380–388. [[CrossRef](#)]
89. Liu, Y.R.; Li, W.G.; Chen, L.F.; Xiao, B.K.; Yang, J.Y.; Yang, L.; Zhanga, C.-G.; Huang, R.-Q.; Dong, J.X. ABTS+ scavenging potency of selected flavonols from *Hypericum perforatum* L. by HPLC-ESI/MS QQQ: Reaction observation, adduct characterization and scavenging activity determination. *Food Res. Int.* **2014**. [[CrossRef](#)]
90. Tai, A.; Ohno, A.; Ito, H. Isolation and Characterization of the 2,2'-Azinobis(3-ethylbenzothiazoline-6-sulfonic acid) (ABTS) Radical Cation-Scavenging Reaction Products of Arbutin. *J. Agric. Food Chem.* **2016**, *64*, 7285–7290. [[CrossRef](#)]
91. Li, W.; Zhang, Y.; Liu, Y.; Yue, F.; Lu, Y.; Qiu, H.; Gao, D.; Gao, Y.; Wu, Y.; Wang, Z.; et al. In vitro kinetic evaluation of the free radical scavenging ability of propofol. *Anesthesiology* **2012**, *116*, 1258–1266. [[CrossRef](#)] [[PubMed](#)]
92. Hilgers, R.; Vincken, J.P.; Gruppen, H.; Kabel, M.A. Laccase/Mediator Systems: Their Reactivity toward Phenolic Lignin Structures. *ACS Sustain. Chem. Eng.* **2018**, *6*, 2037–2046. [[CrossRef](#)] [[PubMed](#)]
93. Arnao, M.B.; Casas, J.L.; del Río, J.A.; Acosta, M.; García-Cánovas, F. An enzymatic colorimetric method for measuring naringin using 2,2'-azino-bis-(3-ethylbenzthiazoline-6-sulfonic acid) (ABTS) in the presence of peroxidase. *Anal. Biochem.* **1990**, *185*, 335–338. [[CrossRef](#)]
94. Marín, F.R.; Hernández-Ruiz, J.; Arnao, M.B. A colorimetric method for the determination of different functional flavonoids using 2,2'-azino-bis-(3-ethylbenzthiazoline-6-sulphonic acid) (ABTS) and peroxidase. *Prep. Biochem. Biotechnol.* **2019**, *49*, 1033–1039. [[CrossRef](#)] [[PubMed](#)]
95. Henriquez, C.; Aliaga, C.; Lissi, E. Kinetics profiles in the reaction of ABTS derived radicals with simple phenols and polyphenols. *J. Chil. Chem. Soc.* **2004**, *49*, 65–67. [[CrossRef](#)]
96. Mira, L.; Silva, M.; Rocha, R.; Manso, C.F. Measurement of relative antioxidant activity of compounds: A methodological note. *Redox Rep.* **1999**, *4*, 69–74. [[CrossRef](#)]
97. Sekher Pannala, A.; Chan, T.S.; O'Brien, P.J.; Rice-Evans, C.A. Flavonoid B-ring chemistry and antioxidant activity: Fast reaction kinetics. *Biochem. Biophys. Res. Commun.* **2001**, *282*, 1161–1168. [[CrossRef](#)]
98. Sentkowska, A.; Pyrzyńska, K. Investigation of antioxidant interaction between Green tea polyphenols and acetaminophen using isobolographic analysis. *J. Pharm. Biomed. Anal.* **2018**, *159*, 393–397. [[CrossRef](#)]
99. Sentkowska, A.; Pyrzyńska, K. Investigation of antioxidant activity of selenium compounds and their mixtures with tea polyphenols. *Mol. Biol. Rep.* **2019**, *46*, 3019–3024. [[CrossRef](#)]
100. Olszowy-Tomczyk, M. Synergistic, Antagonistic and Additive Antioxidant Effects in the Binary Mixtures. *Phytochem. Rev.* **2020**, *19*, 63–103. [[CrossRef](#)]
101. Freeman, B.L.; Eggett, D.L.; Parker, T.L. Synergistic and antagonistic interactions of phenolic compounds found in navel oranges. *J. Food Sci.* **2010**, *75*, 570–575. [[CrossRef](#)] [[PubMed](#)]
102. Heo, H.J.; Kim, Y.J.; Chung, D.; Kim, D.O. Antioxidant capacities of individual and combined phenolics in a model system. *Food Chem.* **2007**, *104*, 87–92. [[CrossRef](#)]
103. Iacopini, P.; Baldi, M.; Storchi, P.; Sebastiani, L. Catechin, epicatechin, quercetin, rutin and resveratrol in red grape: Content, in vitro antioxidant activity and interactions. *J. Food Compos. Anal.* **2008**, *21*, 589–598. [[CrossRef](#)]

104. Peyrat-Maillard, M.N.; Cuvelier, M.E.; Berset, C. Antioxidant Activity of Phenolic Compounds in 2,2'-Azobis (2-amidinopropane) Dihydrochloride (AAPH)-Induced Oxidation: Synergistic and Antagonistic Effects. *J. Am. Oil Chem. Soc.* **2003**, *80*, 1007–1012. [[CrossRef](#)]
105. Wang, S.; Meckling, K.A.; Marcone, M.F.; Kakuda, Y.; Tsao, R. Synergistic, additive, and antagonistic effects of food mixtures on total antioxidant capacities. *J. Agric. Food Chem.* **2011**, *59*, 960–968. [[CrossRef](#)]
106. Nieto, G.; Huvaere, K.; Skibsted, L.H. Antioxidant activity of rosemary and thyme by-products and synergism with added antioxidant in a liposome system. *Eur. Food Res. Technol.* **2011**, *233*, 11–18. [[CrossRef](#)]
107. Chou, T.-C.; Talalay, P. Quantitative analysis of dose-effect relationships: The combined effects of multiple drugs or enzyme inhibitors. *Adv. Enzym. Regul.* **1984**, *22*, 27–55. [[CrossRef](#)]
108. Pereira, R.; Sousa, C.; Costa, A.; Andrade, P.; Valentão, P. Glutathione and the Antioxidant Potential of Binary Mixtures with Flavonoids: Synergisms and Antagonisms. *Molecules* **2013**, *18*, 8858–8872. [[CrossRef](#)]
109. Dawidowicz, A.L.; Olszowy, M. The importance of solvent type in estimating antioxidant properties of phenolic compounds by ABTS assay. *Eur. Food Res. Technol.* **2013**, *236*, 1099–1105. [[CrossRef](#)]
110. Kurin, E.; Mučaji, P.; Nagy, M. In Vitro Antioxidant Activities of Three Red Wine Polyphenols and Their Mixtures: An Interaction Study. *Molecules* **2012**, *17*, 14336–14348. [[CrossRef](#)]
111. Arts, M.J.T.J.; Haenen, G.R.M.M.; Voss, H.P.; Bast, A. Masking of antioxidant capacity by the interaction of flavonoids with protein. *Food Chem. Toxicol.* **2001**, *39*, 787–791. [[CrossRef](#)]
112. Olszowy, M.; Dawidowicz, A.L.; Józwiak-Doleba, M. Are mutual interactions between antioxidants the only factors responsible for antagonistic antioxidant effect of their mixtures? Additive and antagonistic antioxidant effects in mixtures of gallic, ferulic and caffeic acids. *Eur. Food Res. Technol.* **2019**, *245*, 1473–1485.
113. Ilyasov, I.; Beloborodov, V.; Dubrovskaya, A.; Voskoboynikova, I. Flavonoid-ascorbate mixtures ratio-antioxidant activity relationships. *Res. J. Pharm. Biol. Chem. Sci.* **2016**, *7*, 1016–1022.
114. Bors, W.; Michel, C.; Schikora, S. Interaction of flavonoids with ascorbate and determination of their univalent redox potentials: A pulse radiolysis study. *Free Radic. Biol. Med.* **1995**, *19*, 45–52. [[CrossRef](#)]
115. Jones, D.P. Redox potential of GSH/GSSG couple: Assay and biological significance. *Methods Enzymol.* **2002**, *348*, 93–112.
116. Jacobs, H.; Moalin, M.; Bast, A.; van der Vijgh, W.J.F.; Haenen, G.R.M.M. An Essential Difference between the Flavonoids MonoHER and Quercetin in Their Interplay with the Endogenous Antioxidant Network. *PLoS ONE* **2010**, *5*, e13880. [[CrossRef](#)]
117. Boots, A.W.; Kubben, N.; Haenen, G.R.M.M.; Bast, A. Oxidized quercetin reacts with thiols rather than with ascorbate: Implication for quercetin supplementation. *Biochem. Biophys. Res. Commun.* **2003**, *308*, 560–565. [[CrossRef](#)]
118. Awad, H.M.; Boersma, M.G.; Vervoort, J.; Rietjens, I.M.C.M. Peroxidase-Catalyzed Formation of Quercetin Quinone Methide–Glutathione Adducts. *Arch. Biochem. Biophys.* **2000**, *378*, 224–233. [[CrossRef](#)]
119. Awad, H.M.; Boersma, M.G.; Boeren, S.; van Bladeren, P.J.; Vervoort, J.; Rietjens, I.M.C.M. Structure–Activity Study on the Quinone/Quinone Methide Chemistry of Flavonoids. *Chem. Res. Toxicol.* **2001**, *14*, 398–408. [[CrossRef](#)]
120. van der Woude, H.; Boersma, M.G.; Alink, G.M.; Vervoort, J.; Rietjens, I.M.C.M. Consequences of quercetin methylation for its covalent glutathione and DNA adduct formation. *Chem. Biol. Interact.* **2006**, *160*, 193–203. [[CrossRef](#)]
121. Moalin, M.; van Strijdonck, G.P.F.; Bast, A.; Haenen, G.R.M.M. Competition between Ascorbate and Glutathione for the Oxidized Form of Methylated Quercetin Metabolites and Analogues: Tamarixetin, 4'-O-Methylquercetin, Has the Lowest Thiol Reactivity. *J. Agric. Food. Chem.* **2012**, *60*, 9292–9297. [[CrossRef](#)] [[PubMed](#)]
122. Jacobs, H.; Moalin, M.; van Gisbergen, M.W.; Bast, A.; van der Vijgh, W.J.F.; Haenen, G.R.M.M. An essential difference in the reactivity of the glutathione adducts of the structurally closely related flavonoids monoHER and quercetin. *Free Radic. Biol. Med.* **2011**, *51*, 2118–2123. [[CrossRef](#)] [[PubMed](#)]
123. Jacobs, H.; van der Vijgh, W.J.F.; Koek, G.H.; Draaisma, G.J.J.; Moalin, M.; van Strijdonck, G.P.F.; Bast, A.; Haenen, G.R.M.M. Characterization of the glutathione conjugate of the semisynthetic flavonoid monoHER. *Free Radic. Biol. Med.* **2009**, *46*, 1567–1573.
124. Michels, G.; Haenen, G.R.M.; Wätjen, W.; Rietjens, S.; Bast, A. The thiol reactivity of the oxidation product of 3,5,7-trihydroxy-4H-chromen-4-one containing flavonoids. *Toxicol. Lett.* **2004**, *151*, 105–111. [[CrossRef](#)]

125. Galati, G.; Moridani, M.Y.; Chan, T.S.; O'Brien, P.J. Peroxidative metabolism of apigenin and naringenin versus luteolin and quercetin: Glutathione oxidation and conjugation. *Free Radic. Biol. Med.* **2001**, *30*, 370–382. [[CrossRef](#)]
126. Boersma, M.G.; Vervoort, J.; Szymusiak, H.; Lemanska, K.; Tyrakowska, B.; Cenas, N. Regioselectivity and Reversibility of the Glutathione Conjugation of Quercetin Quinone Methide. *Chem. Res. Toxicol.* **2000**, *13*, 185–191. [[CrossRef](#)] [[PubMed](#)]
127. Xie, J.; Schaich, K.M. Re-evaluation of the 2,2-diphenyl-1-picrylhydrazyl free radical (DPPH) assay for antioxidant activity. *J. Agric. Food Chem.* **2014**, *62*, 4251. [[CrossRef](#)]
128. Nenadis, N.; Tsimidou, M.Z. DPPH (2,2-di(4-tert-octylphenyl)-1-picrylhydrazyl) radical scavenging mixed-mode colorimetric assay(s). In *Measurement of Antioxidant Activity & Capacity*; John Wiley & Sons, Ltd.: Chichester, UK, 2017; pp. 141–164.
129. Murakami, M.; Yamaguchi, T.; Takamura, H.; Matoba, T. Effects of ascorbic acid and  $\alpha$ -tocopherol on antioxidant activity of polyphenolic compounds. *J. Food Sci.* **2003**, *68*, 1622–1625. [[CrossRef](#)]
130. González, E.A.; Nazareno, M.A. Antiradical action of flavonoid-ascorbate mixtures. *LWT-Food Sci. Technol.* **2011**, *44*, 558–564. [[CrossRef](#)]
131. MAoun, D.M. Binary mixtures of natural polyphenolic antioxidants with ascorbic acid: Impact of interactions on the antiradical activity. *Int. Food Res. J.* **2012**, *19*, 603–606.



© 2020 by the authors. Licensee MDPI, Basel, Switzerland. This article is an open access article distributed under the terms and conditions of the Creative Commons Attribution (CC BY) license (<http://creativecommons.org/licenses/by/4.0/>).